2015 IEEE Radio & Wireless Week

FINAL PROGRAM

Omni Hotel
San Diego, California, USA
25–28 January, 2015

RWW & RWS General Chair:
Karl Varian

General Co-Chair:
Sergio Pacheco, *Freescale*

RWW & RWS Technical Program Co-Chairs:
Jeremy Muldavin, *MIT Lincoln Laboratory*
Mehdi Shadaram, *University of Texas at San Antonio*

RWW & RWS Finance Chair:
Rashaunda Henderson, *University of Texas at Dallas*

WiSNet Conference Co-Chairs:
Alexander Koelpin, *University of Erlangen-Nuremberg*
Rahul Khanna, *Intel*

PAWR Conference Co-Chairs:
Almudena Suarez Rodriguez, *University of Cantabria*
Fred Schindler, *Qorvo*

BioWireleSS Conference Co-Chairs:
Katia Grenier, *LAAS-CNRS*
Syed Kamrul Islam, *University of Tennessee*

SiRF Conference Chair:
Chien-Nan Kuo, *National Chiao Tung University*

SiRF Technical Program Chair:
Julio Costa, *Qorvo*

SiRF Technical Program Co-Chair:
Hasan Sharifi, *HRL Laboratories*

RWS, PAWR, WiSNet, BioWireleSS Publications Chairs:
Wasif Tanveer Khan, Spyridon Pavlidis, Aida L. Vera Lopez *Georgia Institute of Technology*

SiRF Publication Chair:
Ming-Ta Yang, *Qualcomm*

2015 Radio & Wireless Week Sponsors:
IEEE Microwave Theory and Techniques Society (MTT-S)
IEEE Antennas and Propagation Society (APS)
IEEE Engineering in Medicine & Biology Society (EMBS)

http://www.radiowirelessweek.org

WEDNESDAY, 28 JANUARY 2015

RWW

WiSNet Session: WE1A

Insight in Sensor Networks and System Design

Chair: Rahul Khanna, Intel
Co-Chair: Andreas Stelzer, Johannes Kepler University, Linz

Room: Gallery 1

RWW Session: WE1B

Passive Components and Packaging I

Chair: Hualiang Zhang, University of North Texas
Co-Chair: Roberto Gomez-Garcia, University of Alcala

Room: Grand Salon A

SiRF Session: WE1C

Tunable and Reconfigurable Technologies

Chair: J.P. Raskin, Université catholique de Louvain (UCL)
Co-Chair:Monte Miller, Freescale

Room: Grand Salon B

BioWireleSS Session: WE1D

Micro Biosensing

Chair: Dietmar Kissinger , IHP GmbH
Co-Chair: JC Chiao, University of Texas Arlington

Room: Gallery 2

08:00

WE1A-1 Review of the Present Technologies Concurrently Contributing to the Implementation of the Internet of Things (IoT) Paradigm: RFID, Green Electronics, WPT and Energy Harvesting (Invited)

L. Roselli[1], C. Mariotti[1], P. Mezzanotte[1], F. Alimenti[1], G. Orecchini[1], M. Virili[1], N. B. Carvalho[2], [1]University of Perugia, Perugia, Italy, [2]University of Aveiro, Aveiro, United States

WE1B-1 Miniaturized Via-less Ultra-Wideband Bandpass Filter Based on CRLH-TL Unit Cell

A. O. Alburaikan, M. Aqeeli, X. Huang, Z. Hu, The University of Manchester, Manchester, United Kingdom

WE1C-1 Reconfigurable Solutions for Mobile Device RF Front-ends (Invited)

A. Morris, wiSpry, San Diego, United States

WE1D-1 Why using High Frequency Dielectric Spectroscopy for Biological Analytics? (Invited)

M. Poupot[1,2], D. Dubuc[2,3], F. Artis[1,3], K. Grenier[2,3], J. Fournie[1,2], [1]CRCT , Av. Hubert Curien, France, [2]Univ. Toulouse 3, Toulouse, France, [3]CNRS, Toulouse, France

08:20

WE1A-2 Combined Localization and Data Transmissionin Energy-Constrained Wireless Sensor Networks

T. Nowak[1], A. Koelpin[2], F. Dressler[3], M. Hartmann[1], L. Patino[1], J. Thielecke[2], [1]University of Erlangen-Nürnberg-Inst. Info. Tech., Erlangen, Germany, [2]University of Erlangen-Nürnberg-Inst. Elec. Eng., Erlangen, Germany, [3] University of Paderborn, Paderborn, Germany

WE1B-2 Dual-Band Negative Group Delay Circuit Using Defected Microstrip Structure

G. Chaudhary[1], P. Kim[2], J. Jeong[1], Y. Jeong[1], J. Lim[2], [1]Chonbuk National University, Jeonju-si, Republic of Korea, [2]Soonchunhyang University, Asan, Republic of Korea

08:40

WE1A-3 Wireless Integrated Sensor Nodes for Indoor Monitoring and Localization (Invited)

D. Kissinger[1,2], A. Schwarzmaier[2], F. Grimminger[2], J. Mena-Carrillo[2], W. Weber[2], G. Hofer[2], G. Fischer[2], R. Weigel[2], [1]IHP, Frankfurt (Oder), Germany, [2]Technische Universität Berlin, Berlin, Germany, [3]FAU Erlangen-Nuremberg, Erlangen, Germany, [4]Infineon Technologies, Neubiberg, Germany, [5]Infineon Technologies Austria, Graz, Austria

WE1B-3 A high power Ka-band SPST switch MMIC using 0.25 um GaN on SiC

S. Kaleem[1], J. Kuhn[2], R. Quay[2], M. Hein[1], [1]Ilmenau University of Technology, Ilmenau, Germany, [2]Fraunhofer Society for the Advancement of Applied Research, Freiburg, Germany

WE1C-2 An Integrated Reconfigurable Tuner in 45nm CMOS SOI Technology

A. Jou, C. Liu, S. Mohammadi, Purdue Universty, West Lafayette, United States

WE1D-2 Broadband Dielectric Characterization of CHO-K1 Cells Using Miniaturized Transmission-Line Sensor

N. Meyne[1], G. Fuge[2], S. Hemanth[3], H. K. Trieu[3], A. Zeng[3], A. F. Jacob[1], [1]Technische Universität Hamburg-Harburg-Inst. Hochfreq., Hamburg, Germany, [2]Technische Universität Hamburg-Harburg-Inst. Bioproz. und Biosys., Hamburg, Germany, [3]Technische Universität Hamburg-Harburg-Inst. Mikrosystem., Hamburg, Germany

09:00

WE1A-4 Low-Weight Wireless Sensor Network for Encounter Detection of Bats

M. Hierold[1], S. Ripperger[2], D. Josic[2], F. Mayer[2], R. Weigel[1], A. Koelpin[1], [1]University of Erlangen-Nuremberg, Erlangen, Germany, [2]Museum of Natural History, Berlin, Germany

WE1B-4 High Frequency-Selectivity Impedance Transformer

P. Kim[1], G. Chaudhary[1], J. Park[1], Y. Jeong[1], J. Lim[2], [1]Chonbuk National University, Jeonju, Republic of Korea, [2]Soonchunhyang University, Asan, Republic of Korea

WE1C-3 Ferroelectric MIM Capacitors for Compact High Tunable Filters

R. De Paolis[1], S. Payan[2], M. Maglione[2], G. Guegan[3], F. Coccetti[1], [1]CNRS, Toulouse, France, [2]CNRS, Bordeaux, France, [3]ST-Microelectronics, Tours, France

WE1D-3 A Microwave Sensor Dedicated to Dielectric Spectroscopy of Nanoliter Volumes of Liquid Medium and Flowing Particles

A. Landoulsi, C. Dalmay, A. Bassaudou, P. Blondy, A. Pothier, XLIM, Limoges, France

09:20

WE1A-5 Ad-Hoc Multilevel Wireless Sensor Networks for Distributed Microclimatic Diffused Monitoring in Precision Agriculture

A. Rodriguez de la Concepcion, R. Stefanelli, D. Trinchero, iXem Labs - Politecnico di Torino, Torino, Italy

WE1B-5 A Class of Planar Multi-Band Wilkinson-Type Power Divider with Intrinsic Filtering Functionality

R. Loeches-Sanchez[1,2] D. Psychogiou[2], D. Peroulis[2], R. Gomez-Garcia[1], [1]University of Alcala, Alcala de Henares, Spain, [2]Purdue University , West Lafayette, United States

WE1C-4 10.6 THz Figure-of-Merit Phase-change RF Switches with Embedded Micro-heater

J. Moon, H. Seo, D. Le, H. Fung, A. Schmitz, T. Oh, S. Kim, K. Son, B. Yang, HRL Laboratories, Malibu, United States

WE1D-4 Sub-microliter Microwave Dielectric Spectroscopy for Identification and Quantification of Carbohydrates in Aqueous Solution

F. Artis[1,2], D. Dubuc[1], J. Fournie[2], M. Poupot[2], K. Grenier[4], [1]LAAS-CNRS and Toulouse Univ., Toulouse, France, [2]CRCT, Toulouse, France

Dual-Band Negative Group Delay Circuit Using Defected Microstrip Structure

Girdhari Chaudhary[1], Phirun Kim[1], Junhyung Jeong[1], Yongchae Jeong[1], and Jongsik Lim[2]

[1]Division of Electronics and Information Engineering, Chonbuk National University, South Korea,
[2]Department of Electrical Engineering, Soonchunhyang University, South Korea

Abstract — **This paper demonstrates a design and analysis of a dual-band negative group delay (NGD) network using defected microstrip structure (DMS). The group delays (GD) and signal attenuation (SA) of each band can be controlled independently by resistors connected across U-shaped DMS slots. For the experimental validation, the NGD network is designed and fabricated. For enhancement of the NGD bandwidth, two-stage NGD networks with slightly different center frequencies are connected in cascade. From the measurement, the GDs of -3.86±0.94 ns and -3.26±1.07 ns are obtained at 3.32-3.44 GHz and 4.63-4.76 GHz, respectively.**

Index Terms — **Defected microstrip structure, distributed transmission line, dual-band, negative group delay.**

I. Introduction

Multi-band/mode communication systems are in strong demand to cover several communication standards and provide functionality with a single device. Therefore, the amount of research on the development of multi-band devices has increased.

Since the concept of abnormal group velocity which includes negative group delay (NGD) has proven theoretically in electronic circuitry [1], various works have been performed to design NGD networks at microwave frequencies [2]-[5]. The NGD can occur within limited frequency bands where absorption or signal attenuation (SA) is maximum and can provide the time advancement in wave propagation [1]. The characteristics of the NGD networks have been applied to various practical applications in communication systems [3]-[5].

Recently, there is a growing interest in periodic structures such as microstrip photonic bandgap (PBG), defected ground structure (DGS), and defected microstrip structure (DMS) which provide the SA at a certain resonant frequency and has applied successfully in various applications [6]. In the DMS, the patterned structure is etched on signal strip instead of the ground plane. The SA characteristic of the DMS was used in designing single band NGD network [7]. However, a few studies are focused on the design of dual-band NGD networks [8]-[9]. A dual-band NGD network using a composite right/left handed (CRLH) transmission line is presented in [8]. However, it is not possible to independently control the GD times of both bands.

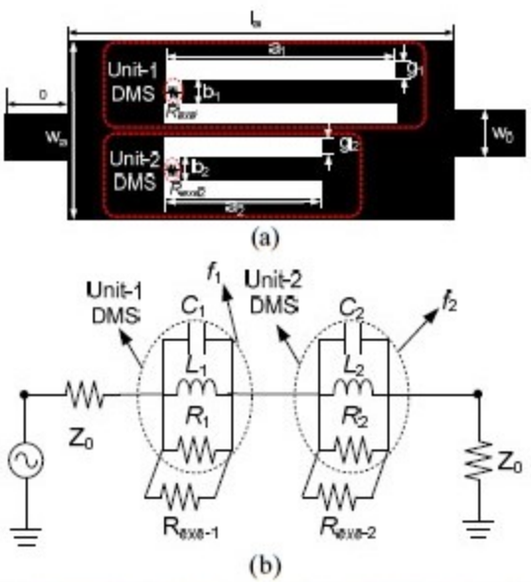

Fig. 1. (a) Proposed structure of dual-band NGD network and (b) equivalent circuit.

In this paper, the SA characteristics of DMS is used to design the dual-band NGD network. In order to get dual-band characteristics, two U-shaped DMS with slightly different dimensions are used. The amount of GD and SA at frequency bands are controlled by external resistors connected in DMS slots.

II. Design and Implementation

Fig. 1(a) shows the structure of proposed dual-band NGD network which consists of two U-shaped DMSs. The unit-1 DMS is used for lower frequency band whereas unit-2 for the higher frequency band. The external resistors are connected in DMS slots in order to get the desired amount of GD time at center frequencies of dual-band. The equivalent circuit of proposed structure is shown in Fig. 1(b). The lumped element values of equivalent DMS are obtained by performing an electromagnetic (EM) simulation [7]. The externally connected R_{exe-1} and R_{exe-2} are equivalently in parallel with the *RLC* circuits of DMS as shown in Fig. 1(b). The added R_{exe-1} and R_{exe-2} are used to get the required transmission characteristics at the each resonant frequency. From the equivalent circuit of proposed structure, the GD and SA at each band can be calculated as (1).

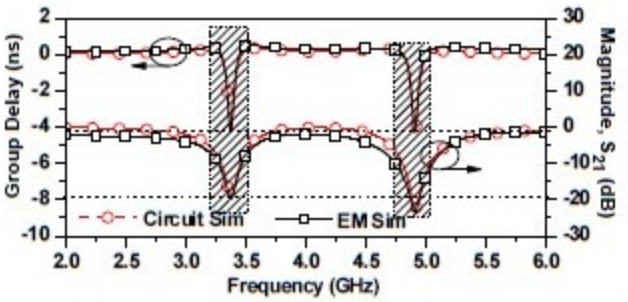

Fig. 2. Simulated group delay (GD) and signal attenuation (SA) characteristics of the dual-band NGD network.

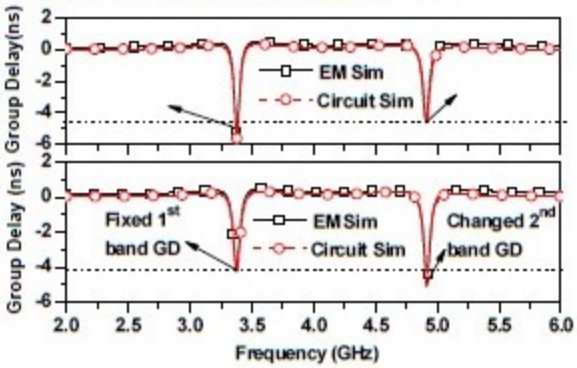

Fig. 3. Simulated group delay characteristics of dual-band NGD network according to different $R_{exe\text{-}1}$ and $R_{exe\text{-}2}$.

$$\tau\big|_{f=f_1,f_2} = -\frac{1}{2\pi}\frac{d\angle S_{21}}{df} = -\frac{2R_{ti}^2 C_i}{2Z_0 + R_{ti}} = \frac{R_{ti}}{\pi\Delta f_i\left(2Z_0 + R_{ti}\right)} \quad (1a)$$

$$S_{21}\big|_{f=f_1,f_2} = \frac{2Z_0}{2Z_0 + R_{ti}}, \quad i = 1,2 \quad (1b)$$

where Z_0 is a termination port impedance. $\Delta f_i = 1/2\pi R_{ti}C_i$ is a 3 dB bandwidth of resonators (DMS) which is lower than the maximum SA for each band. The values of $R_{tot\text{-}i}$ are given as (2).

$$R_{ti} = \frac{R_i R_{exe-i}}{R_i + R_{exe-i}}, i = 1,2 \quad (2)$$

From (1) and (2), it is clear that the GD time can be controlled by $R_{exe\text{-}i}$. To verity the design concept of the proposed NGD, the dual-U-shaped DMS is firstly simulated with an EM solver of Ansoft HFSS v13 with the following dimensions: w_0=2.4, l_0=2, w_a =8, l_a=20, a_1=16, b_1=b_2=2.4, g_1=g_2=0.4, and a_2=10.02 (all units are in mm). The simulation is performed using a substrate RT/Duroid 5880 with a dielectric constant (ε_r) of 2.2 and thickness (h) of 31 mils.

From EM simulation, the 3-dB cut-off and resonant frequencies of first band are determined as 3.155 GHz and 3.38 GHz and of second band 4.59 GHz and 4.91 GHz, respectively. Therefore, the extracted value of equivalent circuit of DMS are given as C_1=3.415 pF, L_1=0.6492 nH, R_1=4.2732 kΩ, C_2=2.403 pF, L_2=0.4363 nH, and R_2= 3.2285 kΩ, respectively. The transmission coefficients (S_{21}) are controlled by connecting $R_{exe\text{-}1}$=4.5 kΩ and R_{exe2}= 3.5 kΩ.

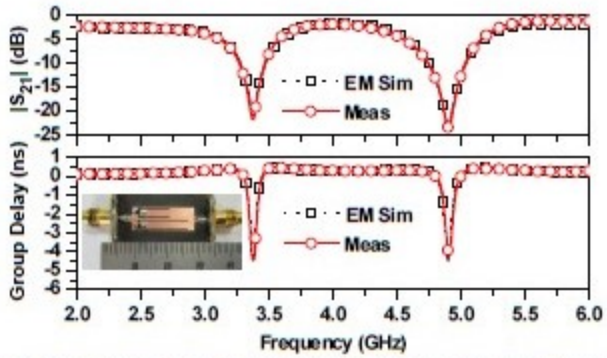

Fig. 4. Simulation and measurement results of 1-stage dual-band NGD network.

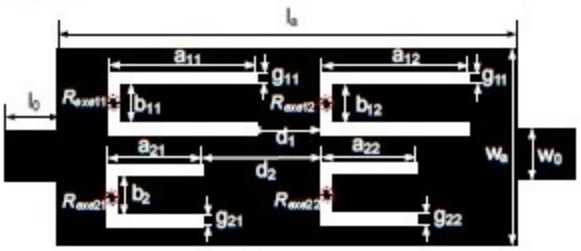

Fig. 5. EM simulation layout of 2-stage dual-band NGD network.

Fig. 2 shows the EM and circuit simulation results of the proposed dual-band NGD network. As shown in figure, the circuit simulation has good agreement with the EM simulation. The center frequencies of the NGD network are located at 3.38 GHz and 4.915 GHz with GD of -4.22 ns, respectively.

Fig. 3 shows the GD simulation results of the proposed NGD network according to different values of external resistors ($R_{exe\text{-}1}$ and $R_{exe\text{-}2}$). As shown in these figures, the GD of each band can be controlled independently with the external resistors.

III. Simulation and Measurement Results

For experimental validation of proposed structure, the design goal was the GD of -4.5 ns at center frequency of 3.38 GHz and 4.90 GHz, respectively. For this purpose, the NGD network with dual U-shaped DMS is simulated, fabricated, and compared with the circuit simulation. The physical dimensions of dual-U-shaped DMS are same the previous.

Fig. 4 shows the simulation and measurement results of dual-band NGD network. The measurement results agree with those of the simulations. From the measurement, the GD time and SA at first band are determined as -4.2 ns and 21.5 dB. Similarly, GD time and SA at second band of 4.91 GHz are measured as -4.22 ns and 23.05 dB. The SA at second band is slightly higher than first band for same GD time because the inductance at the second band is lower than the first band which requires higher value $R_{exe\text{-}2} > R_{exe\text{-}1}$ to get same GD at both bands. Therefore, the higher value of $R_{exe\text{-}2}$ creates high SA as described by (2b).

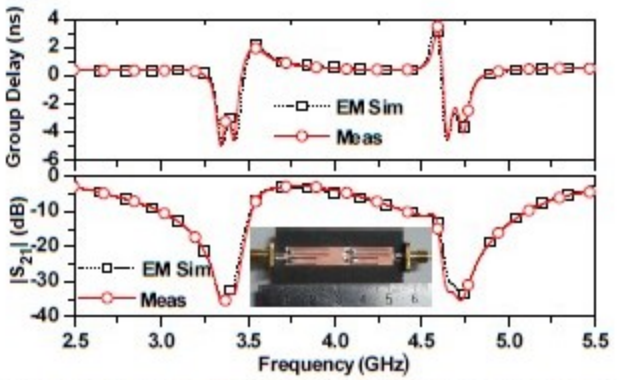

Fig. 6. Simulation and measurement results of 2-stage dual-band NGD network.

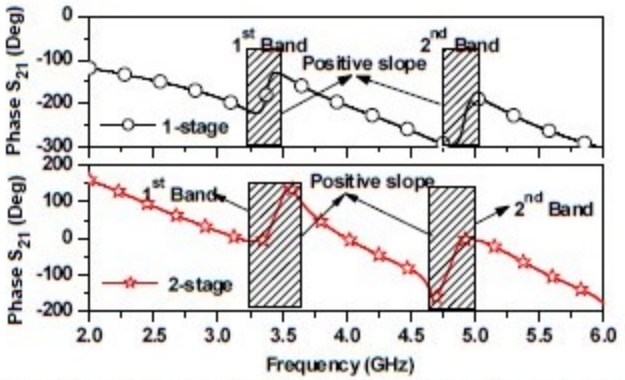

Fig. 7. Measured S_{21} phase characteristics of 1-stage and 2-stage NGD networks.

As seen from Fig. 4, the NGD bandwidth is narrower which show a difficulty to use in the practical applications. Therefore, it is necessary to enhance NGD bandwidth.

One way to increase bandwidth is to cascade NGD networks with slightly different center frequencies as shown in Fig. 5. The physical dimensions of proposed two-stage NGD network are given as $w_0 = 2.4$, $l_0 = 4$, $w_a = 8$, $l_a = 42$, $a_{11} = 16$, $a_{12} = 15.4$, $a_{21} = 11$, $a_{22} = 10.8$, $b_{11} = b_{12} = 2.2$, $b_{21} = b_{22} = 1.8$, $g_{11} = g_{12} = g_{21} = g_{22} = 0.4$, $d_1 = 8$, and $d_2 = 13$ (all units in millimeters). The values of external resistors are given as $R_{exe11} = R_{exe12} = 2.5$ kΩ and $R_{exe21} = R_{exe22} = 4.5$ kΩ.

Fig. 6 shows the EM simulation and measurement results of two-stage NGD network. The measurement results agree with those of the simulations. From the measurement, GD time at first band is obtained as -3.86±0.94 ns for 3.32-3.44 GHz and maximum SA is given as 36.22 dB at center frequency. Similarly, maximum achievable GD time at second band is determined as -3.26±1.07 ns for 4.63-4.76 GHz. The maximum SA at center frequency of second band is obtained as 34.92 dB. The slightly differences in GD and SA are due to chip resistor tolerance and measurement errors.

Fig. 7 shows the phase characteristics of S_{21} of the proposed dual-band NGD networks. As shown in these figures, the phase slope of S_{21} is positive over certain frequency range which signifies the presence of NGD time.

VII. Conclusion

This paper demonstrated the design of dual-band negative group delay networks using dual-U-shaped defected microsrtip structures. The group delay and signal attenuation are controlled by external resistors connected across defected microstrip structure slots. The design concept of the proposed structure is verified with circuit simulation and measurement. The proposed structure has greater freedom in controlling group delay of each band independently. For the experimental validation, dual-band negative group delay networks are designed, simulated, and fabricated. The measurement results are well matched with the simulations. The proposed structure is simple to fabricate and applicable for multi-band communication systems.

Acknowledgement

This work was supported by Basic Science Research Program through the National Research Foundation of Korea (NRF) funded by the Ministry of Education (2014R1A1A2007779).

References

[1] M. Kitano, T. Nakanishi, and K. Sugiyama, "Negative group delay and superluminal propagation: An electronic circuit approach," *IEEE J. Sel. Top. Quantum Electron.*, vol. 9, no. 1, pp. 43-51, Jan. 2003.

[2] G. Chaudhary and Y. Jeong, "Distributed transmission line negative group delay circuit with improved signal attenuation," *IEEE Microw. Wireless Compon. Letters*, vol. 24, no. 1, pp. 20-22, Jan. 2014.

[3] H. Choi, Y. Jeong, C. D. Kim, and J. S. Kenney, "Efficiency enhancement of feedforward amplifiers by employing a negative group delay circuit," *IEEE Trans. Microw. Theory Tech.*, vol. 58, no. 5, pp. 1116-1125, May 2010.

[4] S. S. Oh and L. Shafai, "Compensated circuit with characteristics of lossless double negative materials and its application to array antennas," *IET Microw. Antennas & Propagation*, vol. 1, no. 1, pp. 29-38, Feb. 2007.

[5] H. Mirzaei and G. V. Eleftheriades, "Realizing non-Foster reactive elements using negative group delay networks," *IEEE Trans. Microw. Theory Tech.*, vol. 61, no. 12, pp. 4322-4332, Dec. 2013.

[6] D. Ahn, J. Park, C. Kim, J. Kim, Y. Qian, and T. Itoh, "A design of the low-pass filter using a novel microtrip defected ground structure," *IEEE Tans. Microw. Theory Tech.* vol. 49, no. 1, pp. 86-93, Jan. 2001.

[7] G. Chaudhary, Y. Jeong, and J. Lim, "Miniaturized negative group delay network circuit using defected microstrip structure and lumped elements," *IEEE MTT-S Internatioanl Microw. Sympo. Digest*, pp. 1-3, Jun. 2013.

[8] H. Choi, Y. Jeong, J. Lim, S. Y. Eom, and Y. Jung, "A novel design of a dual-band negative group delay circuut," *IEEE Microw. Wireless Compon. Letters*, vol. 21, no. 1, pp. 19-21, Jan.2011.

[9] B. Ravelo and S. Blasi, "An FET-based microwave active circuit with dual-band negative group delay," *Journal of Microw. Optoelectronics and Electromagn. Applications*, vol. 10, no. 2, pp. 355-366, Dec. 2011.